



**HAL**  
open science

## Electrospun Nanofibre Mats Coating - New Route to Flame Retardancy

Emanuela Gallo, Ziyin Fan, Bernhard Schartel, Andreas Greiner

► **To cite this version:**

Emanuela Gallo, Ziyin Fan, Bernhard Schartel, Andreas Greiner. Electrospun Nanofibre Mats Coating - New Route to Flame Retardancy. *Polymers for Advanced Technologies*, 2011, 22 (7), pp.1205. 10.1002/pat.1994 . hal-00647885

**HAL Id: hal-00647885**

**<https://hal.science/hal-00647885>**

Submitted on 3 Dec 2011

**HAL** is a multi-disciplinary open access archive for the deposit and dissemination of scientific research documents, whether they are published or not. The documents may come from teaching and research institutions in France or abroad, or from public or private research centers.

L'archive ouverte pluridisciplinaire **HAL**, est destinée au dépôt et à la diffusion de documents scientifiques de niveau recherche, publiés ou non, émanant des établissements d'enseignement et de recherche français ou étrangers, des laboratoires publics ou privés.



**Electrospun Nanofibre Mats Coating - New Route to Flame Retardancy**

Journal:	<i>Polymers for Advanced Technologies</i>
Manuscript ID:	PAT-11-009.R1
Wiley - Manuscript type:	Short Communication
Keywords:	electrospinning, polyimide, nanofibres, fire retardancy

SCHOLARONE™  
Manuscripts

Review

**Short Communication:****Electrospun Nanofibre Mats Coating - New Route  
to Flame Retardancy**E. Gallo,<sup>a</sup> Z. Fan,<sup>b</sup> B. Schartel,<sup>a\*</sup> A. Greiner<sup>b</sup><sup>a</sup> BAM Federal Institute for Materials Research and Testing, Unter den Eichen 87, 12205 Berlin,  
Germany<sup>b</sup> Philipps-University Marburg, Department of Chemistry and Scientific Center for Materials  
Science, Hans-Meerwein-Straße, 35032 Marburg, Germany**Abstract**

A novel route towards halogen-free fire retardancy of polymers through innovative surface coating is described. Nanofibre mats based on polyimide are deposited on PA66 through electrospinning. Scanning electron microscopy (SEM) is used to characterize the nanofibres. Cone calorimeter tests were performed to evaluate the fire performance. Due to their low thermal conductivity, electrospun nanofibre mats act not only as sacrificial layers, but also as a protective surface that delays ignition. The effect is influenced by the fibre diameters and the imidization.

**Keywords:** electrospinning; polyimide; nanofibres; fire retardancy

\*Correspondence to: Tel.: +49 30 8104 1021; Fax: 49-30-8104-1617

E-mail: bernhard.schartel@bam.de (B. Schartel)

## Introduction

Since the major trend in the fire retardancy of polymers is to reduce and replace problematic compounds with ecologically friendly additives, fire protection coatings are considered to be a promising and innovative route. Unlike other classical approaches, surface modification processes<sup>[1,2]</sup> do not involve high loadings of additive fire retardants, since the flame retardancy is concentrated exclusively within the surface layer. Furthermore, by using fire protective coating, additives are not incorporated within the material, preventing deterioration of its intrinsic properties (e.g. the mechanical properties) and maintaining easy processibility.

Fire protection coatings, acting through the phenomena of intumescence,<sup>[3]</sup> form an expanded multicellular layer when heated, which protects the underlying material from the action of the heat flux or flame. As a consequence, intumescent coatings must be optimized to work in time to have a fire retardant effect, as they intrinsically belong to a later stage, because it takes time for the protective intumescent layers to form. Thus in contrast to intumescent coatings, a fire protective layer placed at the key position in the material – the interface between the condensed and gas phase – can be effective from the beginning, even in the first stages of decomposition. A “sacrificial” layer can protect a flammable substrate, in particular by delaying its ignition. Nevertheless, once the layer is consumed, the burning of the substrate may no longer be retarded. This means that the sacrificial layers must be efficient or thick enough to provide fire protection. However, a clear increase in time to ignition can be an excellent overall approach for flame retardancy.<sup>[4]</sup>

Covering one polymer by another more temperature-resistant or fire-resistant polymer is indeed a reasonable approach to reducing flammability without using additive flame retardants. Polyimides (PI) are an important group of high-performance polymers, popular in many technological applications due to their excellent thermal behaviour, very good chemical resistance and electrical properties.<sup>[5]</sup> Because of these outstanding properties, PI has found extensive application as fibres, films, coatings and composites. However, many aromatic PI are neither soluble nor fusible because of the high rigidity and conjugation of their backbone. These drawbacks cause difficulties in fabrication and limit their applications.

Ultra-thin polyimide nanofibres are made by means of electrospinning.<sup>[6-9]</sup> The process involves the application of a strong electrostatic field to a stream of polymer precursor solutions and subsequent imidization.<sup>[10]</sup> The electrostatic field creates instabilities in the polymer stream, thereby producing ultrafine fibres, often in the nanoscale range. The low density of collected nanofibre mats, similar to that of foam, can provide an additional good thermal insulation for the underlying material.

1  
2 In this work, a new route for flame retardancy by protective coating has been explored.  
3  
4 By electrospinning and electrospinning followed by thermal treatment, thin films of poly(amic  
5 acid) (PAA)-nanofibre mats and PI-nanofibre mats, respectively, are laid down on PA66  
6 substrates. The fire behaviour and thus the flame retardancy properties are evaluated using the  
7 cone calorimeter. PAA-nanofibre mat and PI-nanofibre mat coated PA66 are compared to PAA-  
8 film and PI-film coated PA66, respectively. Additionally, free standing PI nanofibre fabrics are  
9 investigated to get an insight into the fire behaviour of the nanofibre mats themselves. The  
10 impact of nanofibre thickness as well as imidization of PAA to PI is discussed.  
11  
12  
13  
14  
15  
16  
17  
18  
19

## 20 **Experimental Part**

### 21 *Materials*

22  
23  
24  
25 PA66 (Ultramid, BASF AG, Germany) was used as substrate in the form of plates (100 x  
26 100 x 3 mm). 4,4-oxydianiline (ODA) 98% and pyromellitic dianhydride (PMDA) 97% were  
27 purchased from Alfa Aesar. ODA was recrystallized from toluene and PDMA was sublimated at  
28 250°C before use. N,N-dimethylformamide (DMF) was dried using a molecular sieve and  
29 distilled before use.  
30  
31  
32  
33

### 34 *Synthesis of PI and its precursor*

35  
36  
37 The PI synthesis was conducted in two steps (Fig. 1): the synthesis of the PAA precursor  
38 and the subsequent imidization process of PAA to PI. During the first step the precursor PAA  
39 was synthesized through a polyaddition between equimolar amounts of dianhydride (PMDA) and  
40 diamine (ODA). A 3-necked 250 ml flask equipped with a mechanical stirrer, argon inlet and  
41 outlet was charged with 0.04 mol of ODA and 70.5 ml of DMF. The mixture was stirred under  
42 flow of dry argon until the complete dissolution of solids, and then cooled below 10°C using an  
43 ice bath. An equimolar amount of PMDA (0.04 mol) was added to the reaction solution in  
44 portions. The precursor solution was stirred vigorously at room temperature for 24 h before  
45 being diluted into three different concentrations from 20 to 15 wt%. Three solutions were  
46 prepared, PAA-20, PAA-18 and PAA-15, whereby the last part of the name indicates the  
47 corresponding concentration in wt%. Two additional materials were produced, PAA-film and PI-  
48 film coated PA66 substrates. In both cases the polymer solution was not electrospun, but a thin  
49 film of PAA precursor solution was deposited on the PA66 matrix by solvent evaporation. The  
50 transparent coatings were around 80 µm and 108 µm thick. Corresponding free-standing  
51 nanofibre PI fabrics (100 mm x 100 mm, 0.5 g) were also investigated for comparison.  
52  
53  
54  
55  
56  
57  
58  
59  
60

### *Preparation of electrospun nanofibres and imidization*

The electrospinning process was performed using electric fields of the order of  $100 \text{ kV m}^{-1}$ , from a 15 kV electrical potential applied to a 12 cm gap between the spinneret and a rotating disc collector. All the PAA precursor solutions were processed by electrospinning on rotating PA66 plates. To ensure adhesion between the PA66 substrate and the nanofibres, DMF was spread on the PA66 plates allowing the first electrospun fibres to stick on the surface. The imidization process (referred as second synthesis step) was accomplished by exposing solution-cast or electrospun nanofibre mat coated PA66 plates in a high-temperature furnace, preceded by vacuum-drying the PAA precursors in order to remove any residual solvent. In order to find the ideal imidization conditions, FTIR spectroscopy was used to follow the imidization reaction. During the imidization the intensity of CH-vibration did not change, while the intensity of CO-vibration increased with the degree of imidization. By comparing the relative intensity changes of the characteristic peaks of the CH-bonds and the C=O-bonds, the degree of the imidization was measured. The best conditions were found to be the treatment of the precursor at 453 K for 24 h. The second step related to the imidization reaction is shown schematically in Fig.1.

### *Characterization*

Cone calorimeter (Fire Testing Technology, FTT, UK) according to ISO 5660 was used to characterize the fire behaviour. PA66, PAA-nanofibre mat coated PA66 (PAA-20, PAA-18, and PAA-15), PI-nanofibre mat coated PA66 (PI-20, PI-18, and PI-15), PAA-film coated PA66 (PA-film) and PI-film coated PA66 (PI-film) were investigated. Additionally, free standing PI nanofibre fabrics are investigated to get an insight into the fire behaviour of the nanofibre mats. Samples of 100 mm x 100 mm x 3 mm were first conditioned at 23°C and 50 % r.h. to equilibrium and then irradiated horizontally at a heat flux of  $50 \text{ kW m}^{-2}$ . Specimens were placed in an aluminium tray. The surface of the specimen was exposed to the irradiation at the distance of 25 mm from cone heater. The aluminium trays were placed on refractory fibre blanket on top of a ceramic board. The free-standing PI nanofibre fabrics were additionally placed in a metal wire cage. The wire cage was formed from a 220 mm x 100 mm sheet of steel mesh (1 mm wire with 10 mm mesh size) around a solid template 3 mm x 100 mm x 100 mm. Most of the samples were measured in triplicate, some of the coated only in duplicate due to a lack of specimen. The latter is strictly speaking not according to ISO 5660, but however the reproducibility was convincing in all cases. The results were averaged. Scanning electron microscopy (SEM) was used to analyze the dispersion and the size of the nanofibres prepared from different solutions.

## Results and Discussion

### *Morphology and Diameter*

The morphology and diameter of electrospun fibres are dependent on the processing parameters<sup>[11]</sup> and were investigated by SEM. The images of electrospun nanofibres before and after imidization are illustrated in Fig. 2. The nanofibres were randomly distributed to form a three-dimensional fibrous network. Different fibre diameters were observed. The results are summarized in Table 1. The average diameter of the nanofibres is affected by the concentration of the precursor solution: the higher the solution concentration, the thicker the corresponding diameter of the nanofibres. The presence of beads in PAA-15 electrospun fibres is a common phenomenon when low viscosity solutions (low concentration) of polymer are used. The density of beads was dramatically reduced as the concentration of the solution increased.

### *Fire Behaviour: Visual Observations*

The visual observation of free-standing PI nanofibres fabrics without any substrate in the cone calorimeter gave a hint of the fire behaviour by PI nanofibre mats used for coating PA66. Neither real ignition nor real flaming combustion were observed, but rather a thermo-oxidative decomposition process. The surface of the nanofibre fabrics exhibited only small surface flames and glowing until the nanofibres were completely consumed and no residue remained. It is concluded that the low density and the large surface-area-to-volume ratio causes this fire behaviour characteristics.

PA66 specimen showed the formation of a dark solid skin before ignition. This skin formation was described before for PA66 and ascribed to the thermo-oxidative decomposition of the PA66 surface.<sup>[12]</sup> The subsequent deformation due to large bubbles under this skin was interpreted as anaerobic decomposition since the skin did not increase in thickness. The bubbling resulted in an unsteady gas release and therefore in some uncertainty in the time to ignition. After ignition, even in the well-ventilated conditions of the cone calorimeter, pyrolysis of the condensed phase is essentially anaerobic. The oxidation taking place in the gas phase (flame zone) consumed all oxygen above the specimen surface. All of the investigated materials burned homogeneously and completely with a stable flame zone above a bubbling liquid surface. The intense boiling and bubbling noted during flaming combustion left behind hardly any char.

In the film-coated samples, before ignition, the superficial layer first turned a darker colour and then started melting. Once ignition occurred, a boiling and bubbling liquid consisting

1  
2 of decomposing PA66 and the original film was observed during flaming combustion. The  
3 polymer was completely consumed and no residue was left at the end of burning.  
4

5 The surface behaviour of the electrospun fibre mats coated PA66 (PAA-20, PAA-18,  
6 PAA-15 and PI-20, PI-18, PI-15) was affected by the different surface behaviour. In contrast to  
7 PA66, the superficial electrospun fibre mat layer covered the underlying material, preventing it  
8 from reaching the critical conditions of ignition for some time. This protection resulted in a  
9 significant increase in time to ignition. When the polymer underneath started decomposing, the  
10 produced fuel accumulated under the skin as long as the surface layer was undamaged (Fig. 3a).  
11 When the surface layer cracked, ignition occurred and a kind of flashing was observed (Fig. 3b).  
12 After ignition the polymeric material burned homogeneously with a stable flame (Fig. 3c).  
13 Hardly any char remained after combustion (Fig. 3d). No significant change in the residue  
14 formation was detected among the materials.  
15  
16  
17  
18  
19  
20  
21  
22  
23  
24

#### 25 *Fire Behaviour: Ignitability*

26 The influence on ignitability using the time to ignition ( $t_{ig}$ ) was monitored (Table 2). The  
27 ignition time reported in Table 2 for free-standing nanofibre fabrics (184 s) indicates when the  
28 glowing began. All of the coated PA66 showed  $t_{ig}$  increased compared to PA66. The influence of  
29 three parameters was discussed: 1) nanofibre mats instead of films, 2) imidization comparing  
30 PAA-film and PI-film coated PA66 as well as PAA and PI nanofibre mat coated PA66 specimen  
31 and 3) fibre thickness of the electrospun PAA and PI fibre mat coatings.  
32  
33  
34  
35  
36

37 The different behaviour of nanofibre mat and film coatings on the  $t_{ig}$  is presented in Fig. 4  
38 (heat release rate, HRR, versus time). No improvement on  $t_{ig}$  was achieved for PAA-film coated  
39 PA66 in comparison to PA66. For both series, PAA (4a) and PI (4b), nanofibre mat coatings  
40 performed better than the corresponding film coating: PAA-film ignites after 39 s, while through  
41 the PAA fibre mat series the  $t_{ig}$  is shifted up to 72 s. In the case of PI coated PA66 samples, PI-  
42 film increased the  $t_{ig}$  up to 60 s in comparison to PA66, but again, this effect was bigger for the  
43 corresponding samples with PI nanofibre mat coating (Fig. 4b). In conclusion, specimens coated  
44 with electrospun nanofibre mats perform better than the corresponding film samples with respect  
45 to improving the  $t_{ig}$ . Using nanofibre mats, the original function of the surface layer was  
46 switched from a “sacrificial” one to a protective one thanks to an additional thermal insulation  
47 effect.  
48  
49  
50  
51  
52  
53  
54  
55  
56

57 The effect of the imidization process on the  $t_{ig}$  for the three concentrations investigated is  
58 reported in Table 2. Through imidization, the less stable PAA precursor was converted into the  
59 more thermal stable PI. The formation of a more thermally stable barrier resulted in better  
60 protection of the underlying PA66 material and in a further shift in the  $t_{ig}$ . The influence of fibre

1  
2 diameter on shifting the  $t_{ig}$  for PAA and PI series is presented in Fig 4. In comparison to PA66,  
3 the biggest improvement in time to ignition was achieved with PAA-20 and PI-20. The thicker  
4 the fibres, the bigger the shift in  $t_{ig}$  to later times.  
5  
6  
7

### 8 9 *Fire Behaviour: Heat Release and Smoke*

10  
11 The maximum HRR (PHRR) and the total heat evolved (THE) are two other important  
12 fire behaviour characteristics determining the fire risks. The effective heat of combustion (EHC  
13 = THE/TML, with TML = total mass loss) is a suitable measure for the gas-phase activity. As  
14 the main fire hazard, the production of smoke and CO was also considered. Table 2 summarizes  
15 all of the evaluated cone calorimeter results. Fig. 5 displays the HRR curves of nanofibre fabrics  
16 without substrate (a) and the two different series of investigated nanofibre mat coated materials,  
17 PAA and PI (b,c,d). The shape of the HRR curve gave some insight into the fire behaviour of the  
18 different materials. The HRR of the nanofibre fabrics started decomposing without a real flaming  
19 process and reached an extremely small PHRR of only  $18 \text{ kWm}^{-2}$  at 200 s. Due to the small  
20 quantities measured in the cone calorimeter test for this material, only the  $t_{ig}$ , PHRR and THE  
21 were evaluated and the corresponding uncertainties are reported separately in Table 2. PA66  
22 showed a HRR curve with a maximum corresponding to the PHRR and a shoulder occurring  
23 immediately after ignition. The shape of the curve remained substantially unchanged for the  
24 coated materials. The differences in the heat and smoke release among the materials were  
25 discussed in terms of different parameters.  
26  
27  
28  
29  
30  
31  
32  
33  
34  
35  
36

37  
38 Neither PAA-film coated nor PI-film coated PA66 significantly altered the PHRR in  
39 comparison to PA66 (Fig. 4a, b). Comparing PAA-film coating with the corresponding nanofibre  
40 mat coatings (Fig. 4a) the peak increased slightly in PAA-18 and PAA-20, while no difference  
41 was detected for PAA-15. No important change was observed between the PHRR of PI-film and  
42 PI-nanofibre mat coated series (Fig. 4b). The THE seemed to be slightly higher in the film-  
43 coated samples than the corresponding nanofibre mat-coated ones. EHC, which is normally  
44 decreased by gas-phase mechanisms, was slightly reduced by film coating in comparison to fibre  
45 mats. As regards uncertainty, the amount of smoke release is unchanged between nanofibres and  
46 the film samples.  
47  
48  
49  
50  
51  
52

53  
54 The PHRR of PA66 was not reduced by imidization of PAA-coatings to PI-coatings, as  
55 depicted for the three sets of materials in Fig. 5 (b,c,d). PHRR of PI samples was always higher  
56 than for the corresponding PAA samples. The higher thermal resistance of the PI-nanofibre mat,  
57 in comparison to the corresponding PAA-nanofibre one, delayed the ignition time. Before  
58 ignition, the material underneath is preheated and begins decomposing. Fuel accumulates under  
59 the surface layer. A prolonged time to ignition implies that the preheated material and gaseous  
60

1  
2 decomposition products have more time to accumulate under the protective layer. This  
3 accumulation resulted in an increased reaction when the superficial layer broke and ignition  
4 occurred. This effect is proposed to be responsible also for the higher PHRR in comparison to  
5 PAA samples. On the contrary, early ignition of PA66 resulted in a lower accumulation of  
6 combustible vapours to yield a lower PHRR after ignition. The near-constant THE and EHC  
7 suggested an unchanged decomposition mechanism with respect to the effective heat of  
8 combustion of the volatiles. No particular effect was detected on the smoke production  
9 parameters.  
10  
11

12  
13  
14  
15  
16 The fibre diameter had an influence on the PHRR (Fig. 4). In comparison to PA66, the  
17 PHRR was clearly increased in the PAA series with increasing fibre diameter (up to 20% in  
18 PAA-20). In the PI series this trend was no longer so clear, as PI-15 has a higher PHRR than PI-  
19 18 and PI-20. The diameter of the fibres did not affect other parameters like fire load (THE),  
20 EHC and smoke; however, minor effects on the order of  $\pm 10\%$  variation were observed.  
21  
22  
23  
24  
25

### 26 27 *Fire Behaviour: Flame Spread Indices*

28  
29 Fire growth rate (FIGRA), maximum average rate of heat emission (MAHRE) and  
30  $\text{PHRR}/t_{\text{ig}}$  are three fire safety engineering indices introduced as measures to assess the main  
31 hazards of developing fires. FIGRA is the largest slope in the HRR *versus* time, which is  
32 believed to represent the propensity of the material for fire growth. The MAHRE index was used  
33 to assess materials, taking into account the HRR and the total heat release (THR) over time.  
34  $\text{PHRR}/t_{\text{ig}}$  was proposed empirically since PHRR and  $t_{\text{ig}}$  may well account for the two  
35 characteristics controlling flame spread: HRR of the burning area and ease of ignition of the  
36 surrounding area. All three of these indices concentrate relevant information into a single  
37 number, which is clearly an oversimplification.<sup>[13]</sup> The calculated values for FIGRA (in this case  
38 estimated as  $\text{PHRR}/\text{time to peak}$ ), MAHRE and  $\text{PHRR}/t_{\text{ig}}$  are presented in Table 2 and provide a  
39 qualitative ranking of the fire hazard of the materials. In comparison to PA66, in all of the coated  
40 materials a general reduction in the propensity for fire growth and flame spread was observed.  
41  
42  
43  
44  
45  
46  
47  
48  
49

50  
51 Compared to PA66, for the PAA-film-coated PA66, FIGRA and  $\text{PHRR}/t_{\text{ig}}$  remained  
52 unchanged; only MAHRE showed a reduction of 20%. For the PI-film, a slight reduction in  
53 FIGRA occurred (12%), whereas MAHRE was decreased by 30% and  $\text{PHRR}/t_{\text{ig}}$  by 35%. The  
54 reduction in MAHRE was larger for the films than for the nanofibre mats due to the increased  
55 PHRR increasing the AHRE. In contrast FIGRA and  $\text{PHRR}/t_{\text{ig}}$  took advantage of the delayed  $t_{\text{ig}}$   
56 and heat release, respectively. A further decrease was observed when the nanofibre mat layer  
57 was used instead of the film for both PAA-nanofibre and PI-nanofibre coated samples. The  
58 reduction observed for PAA nanofibre mat coatings was up to 28% in FIGRA, and 45% in  
59  
60

1  
2 PHRR/ $t_{ig}$ . The reduction observed for PI nanofibre mat coatings was up to 18% in FIGRA, and  
3  
4 50% in PHRR/ $t_{ig}$ . Compared to PA66, the PI-film coating reduced all indices clearly more than  
5  
6 the PAA-film, again indicating the benefit of imidization. In contrast, comparing PAA and PI-  
7  
8 nanofibre mat coated samples reveals a rather muddled role of imidization, in the same order of  
9  
10 magnitude as the uncertainty. Whereas using nanofibre mat coatings has a clear flame retardancy  
11  
12 effect compared to PA66 with respect to all indices, the fibre diameter hardly had a significant  
13  
14 effect in the flame spread indices. Some tendency toward decreasing flame retardancy occurred  
15  
16 for PAA-nanofibre, and toward an increasing one for PI-nanofibre mats with increasing fibre  
17  
18 thickness.

## 19 20 Conclusions

21  
22 PAA based on reacting PMDA and ODA were successfully electrospun using  
23  
24 concentrations in the range from 15 to 20 wt% on PA66 substrates forming a thin superficial  
25  
26 nanofibre mat layers. By thermal treatment they were transformed into PI nanofibre mat  
27  
28 coatings. The fire behaviour was investigated by means of cone calorimeter and compared to  
29  
30 free-standing PI nanofabrics, PA66 and PA66 coated with PAA and PI films, respectively. The  
31  
32 formation of a thin protective layer consisting of nanofibre mat has its main effect in delaying  
33  
34 the  $t_{ig}$ . The data deliver no hint of a change in the chemical processes in the gas and condensed  
35  
36 phase reducing the fire hazard of the underlying PA66. The nanofibre mat coatings are  
37  
38 concluded to work via physical effects changing the mass or heat transport between the pyrolysis  
39  
40 and the flame zone. In comparison to the corresponding film coated PA66 it became clear that  
41  
42 the PAA and the PI nanofibre mat coatings are not only sacrificial, but also protective layers due  
43  
44 to advanced thermal insulation. Different parameters affect the delay in ignition. Imidization of  
45  
46 PAA to PI increases the thermal stability of the coatings, resulting in an enhanced delay in  $t_{ig}$ .  
47  
48 Increasing the PAA precursor concentration increased the fibre diameter within the electrospun  
49  
50 PAA and PI nanofibre mats and resulted in a further increase.

51  
52 Of course the achieved delay in ignition in the investigated systems is probably not large  
53  
54 enough to offer sufficient flame retardancy with respect to commercial exploitation. Increasing  
55  
56 the shift in  $t_{ig}$ , additional reduction in PHRR or the combination with established flame  
57  
58 retardants are obvious next steps of development when following this new approach presented  
59  
60 here the first time. In this regard, it should be noted that the low density and large surface-area-  
to-volume ratio of PI nanofibre fabrics and PI nanofibre mat coatings, respectively, result in  
smouldering-like fire behaviour. On one hand this fire behaviour is an advantage with respect to  
fire risks such as HRR. On the other hand it is accompanied by a thermo-oxidative pyrolysis of  
the PAA and PI nanofibre mats without forming any residual protective layer. In contrast to what

1  
2 was expected from the charring fire behaviour of PI, the PI nanofibre mats did not show any  
3 potential to decrease the PHRR of PA66 pyrolysis to a later stage.  
4

5  
6 However, the increase in  $t_{ig}$  and the discussion on different indices believed to indicate  
7 flame spread and fire growth rate, respectively, underline the potential of the concept already.  
8 The use of electrospun nanofibre mat coatings is proposed as a promising new route to improve  
9 the fire retardancy of polymers.  
10  
11  
12

## 13 14 15 16 17 18 19 20 21 22 23 24 25 26 27 28 29 30 31 32 33 34 35 36 37 38 39 40 41 42 43 44 45 46 47 48 49 50 51 52 53 54 55 56 57 58 59 60

### References

- [1] S. Bourbigot, C. Jama, M. Le Bras, R. Delobel, *Polym. Degr. Stab.* 1999 ; 66 , 153.  
[2] B. Scharrel, G. Kuhn, R. Mix, J. Friedrich, *Macromol. Mater. Eng.* 2002 ; 287 , 579.  
[3] H.L. Vandersall, *J. Fire Flammability* 1971 ; 2 , 97.  
[4] E. Wenz, T. Eckel, B. Scharrel, U. Beck, A. Hertwig, M. Weise, J. Strümpfel, E. Reinhold,  
Patent n. WO/2006/131229.  
[5] P.M. Hergenrother, *High Perform. Polym.* 2003 ; 15 , 3.  
[6] D.H. Reneker, I. Chun, *Nanotechnology* 1996 ; 7 , 216.  
[7] C. Nah, S.H. Han, M.H. Lee, J.S. Kim, D.S. Lee, *Polym. Int.* 2003 ; 52 , 429.  
[8] A. Greiner, J.H. Wendorff, *Angew. Chem. Int. Ed.* 2007 ; 46 , 5670.  
[9] R. Dersch, M. Graeser, A. Greiner, J.H. Wendorff, *Aust. J. Chem.* 2007 ; 60 , 719.  
[10] D.H. Reneker, A.L. Yarin, H. Fong, S. Koombhongse, *J. Appl. Phys.* 2000 ; 87 , 4531.  
[11] A. Frenot, I.S. Chronakis, *Curr. Opin. Colloid. Interface Sci.* 2003 ; 8 , 64.  
[12] B. Scharrel, R. Kunze, D. Neubert, *J. Appl. Polym. Sci.* 2002 ; 83 , 2060.  
[13] B. Scharrel, T.R. Hull, *Fire Mater.* 2007 ; 31 , 327.

## Tables

Table 1 Diameter of fibres for the investigated samples

Sample	Fibre diameter (nm)
PAA-20	$395 \pm 92$
PAA-18	$312 \pm 94$
PAA-15	$107 \pm 32$
PI-20	$378 \pm 98$
PI-18	$308 \pm 82$
PI-15	$109 \pm 32$

**Table 2** Cone calorimeter results (irradiance 50 kWm<sup>-2</sup>)

	<b>t<sub>ig</sub></b>	<b>PHRR</b>	<b>THE</b>	<b>EHC</b>	<b>TSR</b>	<b>CO</b>	<b>FIGRA</b>	<b>MAHRE</b>	<b>PHRR/t<sub>ig</sub></b>
	s	kWm <sup>-2</sup>	MJm <sup>-2</sup>	MJm <sup>-2</sup> g <sup>-1</sup>	m <sup>2</sup> m <sup>-2</sup>	kg/kg	kW/m <sup>2</sup> s	kWm <sup>2</sup>	kWm <sup>-2</sup> s <sup>-1</sup>
<i>Error</i>	± 2	± 50	± 2	± 0.02	± 250	± 0.002	± 0.8	± 25	± 0.8
PI nanofibre fabrics	184	18± 5	1± 0.5	-	-	-	-	-	-
PA66	38	1230	97	2.87	811	0.021	9.3	520	32.4
PAA-film	39	1257	105	2.52	805	0.011	9.5	412	32.2
PAA-15	61	1086	95	2.80	756	0.018	6.7	420	17.8
PAA-18	70	1327	98	2.88	669	0.017	7.8	475	18.9
PAA-20	72	1481	99	2.91	673	0.020	7.7	448	20.6
PI-film	60	1276	105	2.80	776	0.014	8.2	382	21.3
PI-15	75	1447	103	3.06	663	0.019	7.9	492	19.3
PI-18	71	1322	98	2.92	693	0.019	8.6	468	18.6
PI-20	85	1363	99	2.92	810	0.019	7.6	452	16.0

## Figure captions

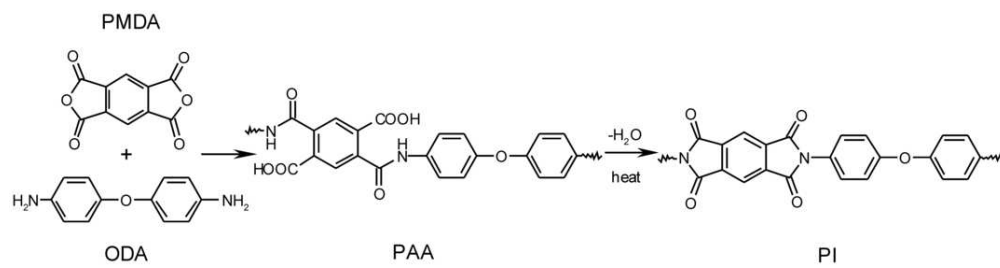
**Figure 1.** Schematic diagram of condensation between dianhydride PMDA and diamine ODA to form the corresponding polyamic acid (PAA), as well as the imidization of PAA into a polyimide (PI).

**Figure 2.** SEM pictures (from left to right) of: PAA-20, PAA-18, PAA-15 (first row) and PI-20, PI-18, PI-15 (second row).

**Figure 3.** Burning behaviour during cone calorimeter experiment for modified PA66 samples.

**Figure 4.** Cone calorimeter results: comparison between film and nanofibres for PA66 and a) PAA-film and PAA-15, PAA-18, PAA-20 and b) PI-film and PI-15, PI-18 and PI-20.

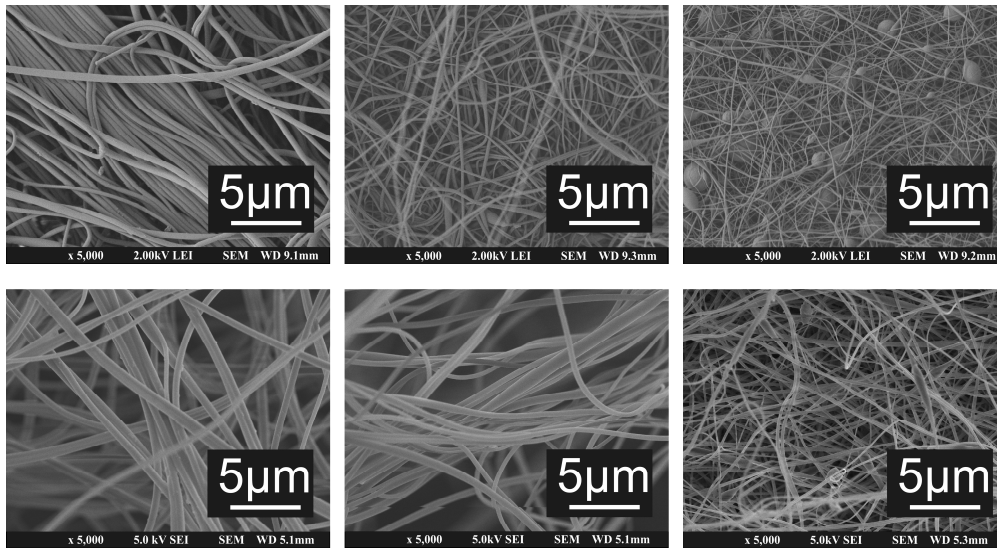
**Figure 5.** Cone calorimeter: heat release rate curve for a) nanofibres; PA66 and b) PAA-15 and PI-15; c) PAA-18 and PI-18; d) PAA-20 and PI-20.



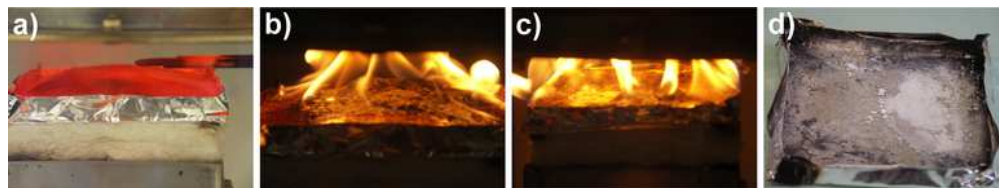
45x11mm (600 x 600 DPI)

For Peer Review

1  
2  
3  
4  
5  
6  
7  
8  
9  
10  
11  
12  
13  
14  
15  
16  
17  
18  
19  
20  
21  
22  
23  
24  
25  
26  
27  
28  
29  
30  
31  
32  
33  
34  
35  
36  
37  
38  
39  
40  
41  
42  
43  
44  
45  
46  
47  
48  
49  
50  
51  
52  
53  
54  
55  
56  
57  
58  
59  
60



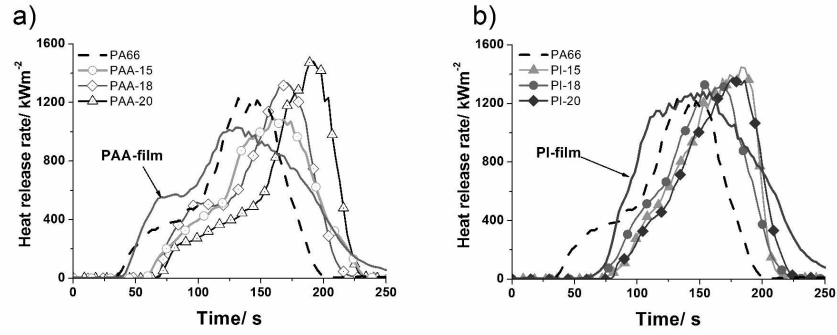
533x289mm (300 x 300 DPI)



32x6mm (600 x 600 DPI)

For Peer Review

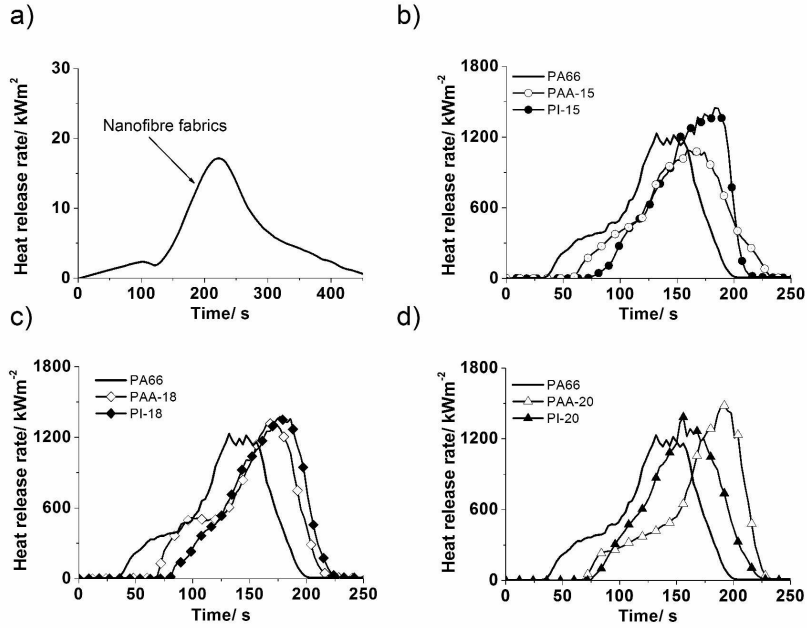
1  
2  
3  
4  
5  
6  
7  
8  
9  
10  
11  
12  
13  
14  
15  
16  
17  
18  
19  
20  
21  
22  
23  
24  
25  
26  
27  
28  
29  
30  
31  
32  
33  
34  
35  
36  
37  
38  
39  
40  
41  
42  
43  
44  
45  
46  
47  
48  
49  
50  
51  
52  
53  
54  
55  
56  
57  
58  
59  
60



177x124mm (600 x 600 DPI)

Review

1  
2  
3  
4  
5  
6  
7  
8  
9  
10  
11  
12  
13  
14  
15  
16  
17  
18  
19  
20  
21  
22  
23  
24  
25  
26  
27  
28  
29  
30  
31  
32  
33  
34  
35  
36  
37  
38  
39  
40  
41  
42  
43  
44  
45  
46  
47  
48  
49  
50  
51  
52  
53  
54  
55  
56  
57  
58  
59  
60



177x125mm (600 x 600 DPI)